

# **Measurement of Gain Stability of a Cryogenic W-band Amplifier Using a Thermal Noise Source**

*J.D. Gallego, I. López Fernández, C. Diez González,  
I. Malo Gómez, R. Amils.*

*IT-CDT 2022-12*

*Observatorio de Yebes  
Apdo. 148 19080  
Guadalajara, SPAIN*



### Change Record

Revision	Date	Affected Paragraphs(s)	Reason/Initiation/Remarks
A	2022-12-04	All	First Issue



## TABLE OF CONTENTS

1. Abstract .....	4
2. Equipment .....	4
3. Setup .....	4
4. Noise Bandwidth .....	7
5. SNGF Measurement Results .....	9
6. Allan Variance Calculation .....	9
7. Conclusions .....	12
8. References .....	12
9. Appendix I: 8474C Diode Detector Data Sheet .....	13

## 1. Abstract

This report presents the method used and the results obtained from the gain fluctuations measurements of a prototype W-band cryogenic amplifier built at Yebes (YMWN 2003). This unit is almost identical to the amplifiers presently in use in the W receivers of the 40m Yebes antenna. The Spectrum of Normalized Gain Fluctuations (SNGF) has been measured over a seven decade Fourier frequency range ( $\approx 2 \cdot 10^{-3} - 2 \cdot 10^4$  Hz). The difference from previous measurements of this type performed in our laboratory is that this time the input signal is broadband noise generated by a thermal load at the input of the amplifier and the values obtained correspond to a weighted average over the pass band of the system. In previous measurements we had always used a low noise, very stable, signal generator at the input and the values obtained corresponded to the CW frequency set. As a suitable generator was not readily available for W-band we decided to use this alternative. The drawback is that with the configuration used it was impossible to independently characterize and then discount the contributions of some active elements of the signal chain (downconverter and IF amplifier). However, it is believed that such contributions should be small at least in the mid-high range of the measured Fourier frequency.

## 2. Equipment

- Agilent 35670A FFT Dynamic Signal Analyzer, DC-102.4 kHz
- Signal Recovery DC Pre-amp Model 5113
- Agilent 8474C Planar-Doped Barrier Diode Detector, 0.01 - 33 GHz
- NP2-12 Sealed Lead Acid Battery 12 V 2Ah
- WR10MixAMC Mixer/Amplifier/Multiplier Chain 70-116 GHz
- Agilent 8257D 50 GHz Analog Signal Generator
- MITEQ Low Noise Amplifier 1-26.5 GHz 30 dB
- Keysight E4412A Wide Dynamic Range Power Sensor, 0.01-18 GHz
- Keysight N1914A EPM Series Dual-Channel Power Meter
- Keysight N8975B Noise Figure Analyzer, 10 MHz - 26.5 GHz (used in the Spectrum Analyzer mode)

## 3. Setup

The setup used is shown schematically in figure 1 and some pictures of the practical implementation are presented in figures 2 and 3. The DUT is a waveguide cryogenic amplifier (YMWN 2003) inside a cryostat with a Sumitomo 4 K cooler and a Lake Shore PID temperature controller with two independent loops. The temperature of the **amplifier** body is sensed and stabilized to **15 K** using heaters located in the cold plate. The input is connected to a W-band waveguide load of the type used for heated load noise measurements similar to the one described in [1]. The temperature of the **load** is sensed and stabilized at **100 K** by the second loop of the controller. The output of the cryostat is connected to a Virginia Diodes downconverter through a waveguide isolator (see figure 2). There is a x4 multiplier built in the downconverter module as well as a low gain ( $\approx 10$  dB) IF amplifier. The Local Oscillator signal is generated by an external synthesizer (not shown in the pictures) set to 23.75 GHz ( $95 \text{ GHz} / 4$ ) and 18 dBm output power. The IF signal further amplified by a MITEQ 30 dB amplifier with the output connected directly to the detector diode. This configuration was chosen to obtain a total power of  $\approx 20$  dBm at the input of the detector. This ensures that the

detector still operates in the quadratic zone (although at the limit) and maximizes the signal-to-noise ratio.

As the detector DC output voltage is only of a few mV it is convenient to amplify it with a low noise DC preamplifier connected by a short cable, trying to avoid as much as possible the interference from the omnipresent 50 Hz grid. The preamplifier is run on batteries to avoid ground loops. Its gain is set to 250 (ambient measurements) or 500 (cryogenic measurements) without filters, obtaining an output of  $\approx 3V$ . The input is DC coupled to make possible measurements at Fourier frequencies below 0.1 Hz (which would be killed by the AC HPF). The output of the preamp is connected to the FFT Analyzer input set to DC, floating ground and fixed scale.

For the measurement of the contribution to the fluctuations of the preamplifier and the FFT analyzer, including its drift and white and quantization noise, a lead-acid battery connected to a resistive voltage divider was employed (see figure 3). The divider was adjusted to provide the same voltage as the detected signal and an output impedance which reproduced that of the video output of the detector. The divider was connected at the input of the preamplifier instead of the detector diode. Measurements of the background were taken at all the sampling rates used for the measurements of the SNGF taking care of using the same gain on the preamp and the same scale of the ADC of the FFT analyzer. The final SNGF was corrected by subtracting this contribution.

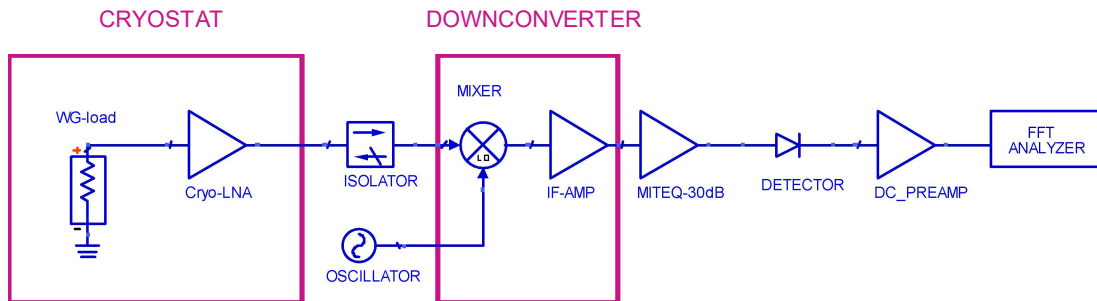


**Figure 1:** Schematic representation of the measurement setup.



**Figure 2:** Up: Test setup used for the measurements. Down: Details of the Virginia Diodes Converter with isolator at the input and MITEQ amplifier and detector connected directly at the output.

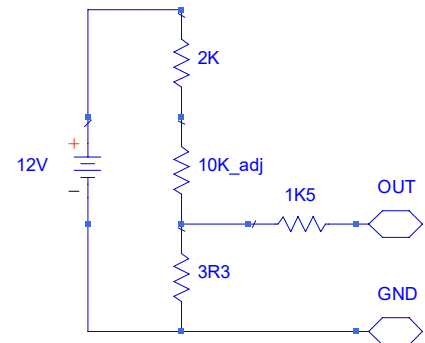
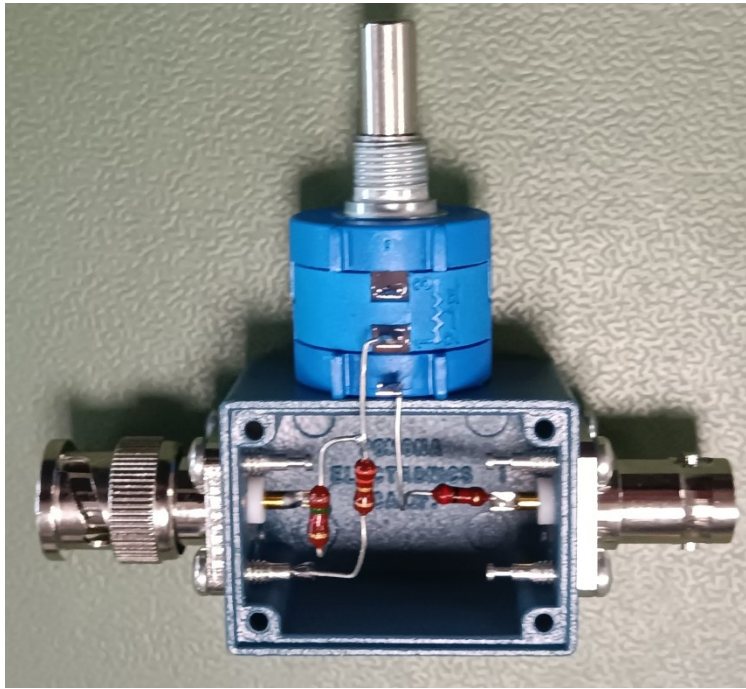


**Figure 3:** View of the low noise resistive divider used for the measurement of the background of the pre-amp and FFT analyzer. It incorporates only metallic film resistors and a 10 turn precision wirewound potentiometer.

## 4. Noise Bandwidth

The IF noise spectrum at the input of the power detector was measured with a microwave spectrum analyzer and the results, including the corrections introduced subtracting the background and taking into account the connecting cable loss are shown in figure 4. Note that there is a quite significant slope and ripple, but the response extends up to  $\approx 20$  GHz. From the decibel data, the linear response is obtained and used to calculate the effective noise bandwidth as:

$$NBW = \int_0^{\infty} \frac{P(f)}{P_{\max}} df$$

Were  $P(f)$  is the measured power spectrum and  $P_{\max}$  its maximum value. Then, the noise bandwidth can be understood as the cutoff frequency of a hypothetical brickwall spectrum with the same maximum value and with the condition that both (measured and brickwall) have same integrated noise power. This is illustrated in figure 4.

Note that the power spectrum is measured at the IF output, but the converter of figure 1 is DSB (no image rejection filter). Then, assuming equal conversion loss for the two sidebands, the noise bandwidth at the input frequency is twice the value obtained at the IF. Since the **LO** frequency is **95 GHz** and the **IF** noise bandwidth obtained is 5.665 GHz, the total noise bandwidth referred to the input is **11.330 GHz** and the value of the gain fluctuation obtained will be a weighted average over the **89.335-100.665 GHz** frequency range.

The total IF noise power at the input of the detector was measured independently with a wide band calibrated diode power detector and the result was -21 dBm (cryogenic) and -20 dBm (ambient).

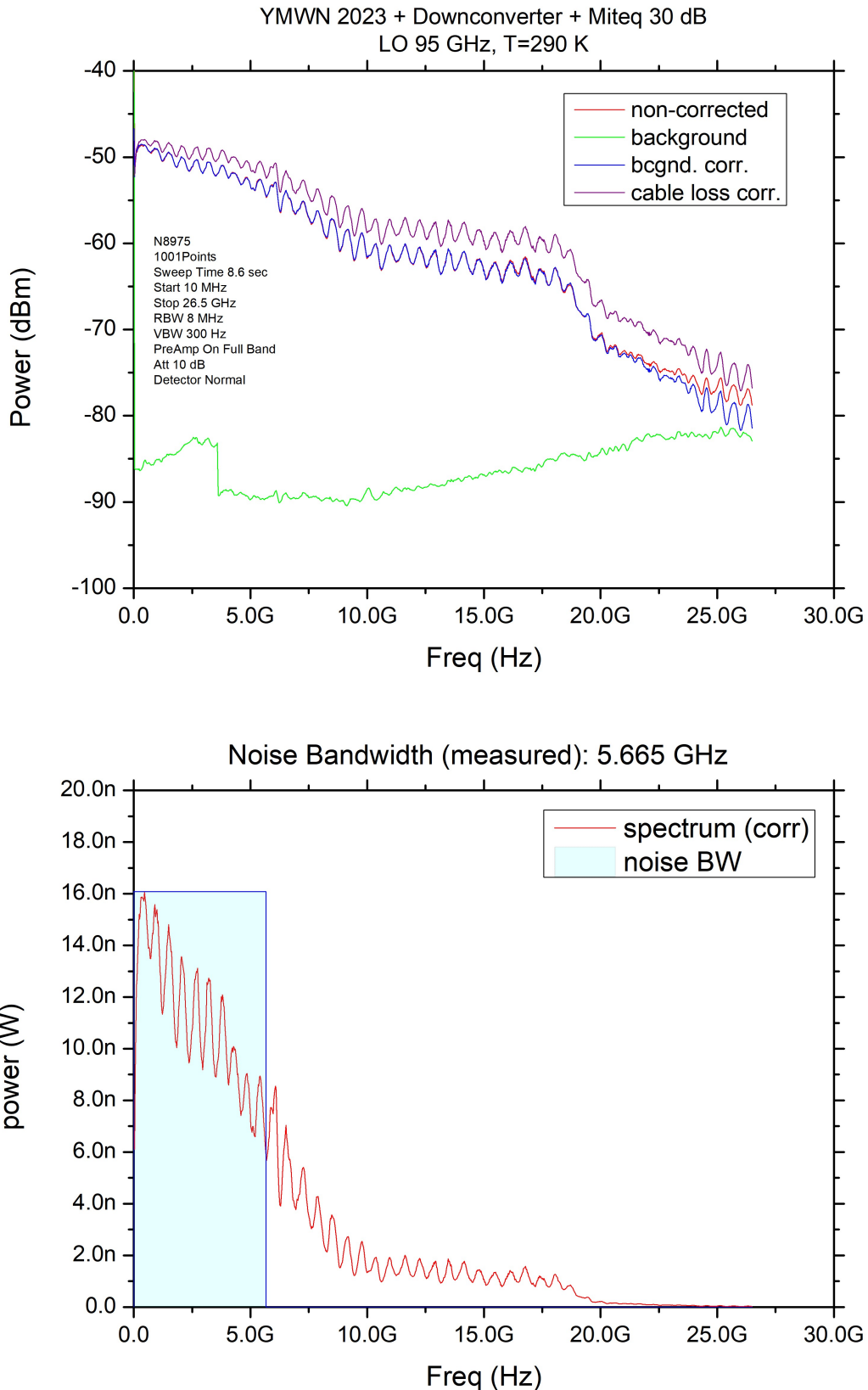


**Figure 4:** Spectrum Analyzer measurement of noise power at the input of the detector. UP: Logarithmic power scale (dB) and corrections applied (subtraction of background and cable loss). DOWN: Power in linear scale and calculated noise bandwidth obtained by integration shown in the same graph for comparison. The value obtained for the noise bandwidth is 5.665 GHz.



## 5. SNGF Measurement Results

The measurement of the SNGF was performed by acquiring the time domain data with the Dynamic Signal Analyzer, storing it in computer files, and using MathCAD to compute the FFT and the average of a number of spectra ( $n=50$ ). This method is more flexible than just reading the FFT calculated by the instrument since it allows independent inspection of each acquisition and complete control of the math involved. The time domain scans were taken with 4096 points and total times of 0.0625, 1, 16, 64 and 512 seconds to obtain a good frequency coverage spanning over 7 decades. The contribution of the preamplifier and FFT analyzer was subtracted from the spectra. The gain of the preamplifier was set to 250 at ambient and 500 at cryogenic temperature to keep a similar power level at the input of the FFT Analyzer. The composite SNGF at ambient and cryogenic temperature is shown in Figure 5 along with the expressions fitted to model it. The cryogenic temperature plot also shows the background contribution from the preamp and FFT analyzer as well as the expected white noise level according with the measured noise bandwidth.

Note that the fitted functions of the ambient and cryogenic measurements differ mainly in the value of the  $f^{-1/2}$  coefficient which is larger in the cryogenic case while the coefficients of white noise and  $1/f$  noise are similar. As seen in figure 5 the white noise component agrees well with the value calculated from the measured noise bandwidth  $(2/NBW)^{1/2}$  and this does not change significantly when the amplifier is cooled. From experience in the measurement of the SNGF of cryogenic amplifiers with CW signals at lower frequencies [2], usually the dominant term appearing is only the one of  $f^{-1/2}$ . In this sense, the coefficient obtained in the present measurement can be considered good for a four stage amplifier. This coefficient is worse by a factor of about 2 at cryogenic temperature, which is also normal based on this experience. The existence of the  $1/f$  term which remains almost constant at ambient and cryogenic temperature makes us suspect that perhaps is caused by the contribution of the converter and the IF amplifier and not to the W-band amplifier. Further research may be needed to clarify this point.

## 6. Allan Variance Calculation

As shown in the previous section, The SNGF measured can be fitted by an expression of the form:

$$SNGF(f) = \sqrt{\frac{2}{NBW}} + bf^{-1/2} + cf^{-1}$$

Were  $NBW$  is the noise bandwidth,  $f$  is the Fourier frequency and  $b$  and  $c$  the coefficients. It can be shown [2] that the Allan Variance (AVAR) of that can be obtained analytically by the expression:

$$AVAR(\tau) = \frac{1}{NBW} \tau^{-1} + 2 \ln(2) b^2 + \frac{2}{3} \pi^2 c^2 \tau$$

In practice the SNGF is only known in a limited frequency range ( $f_{\min}$ ,  $f_{\max}$ ).

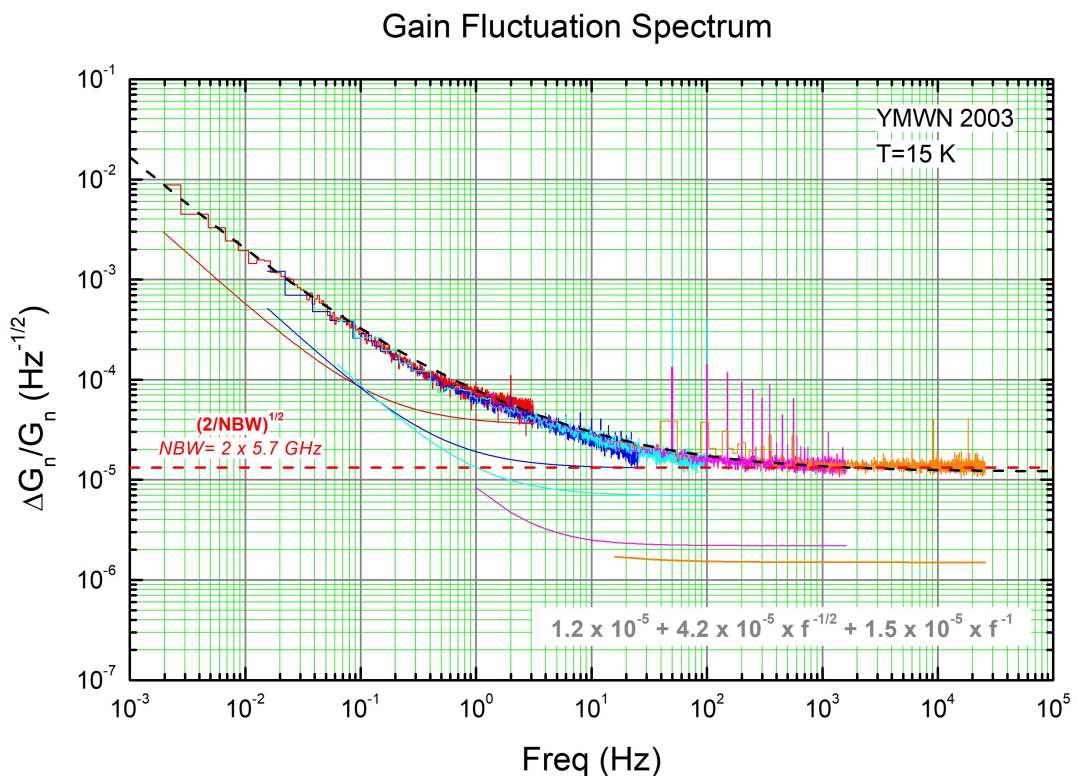
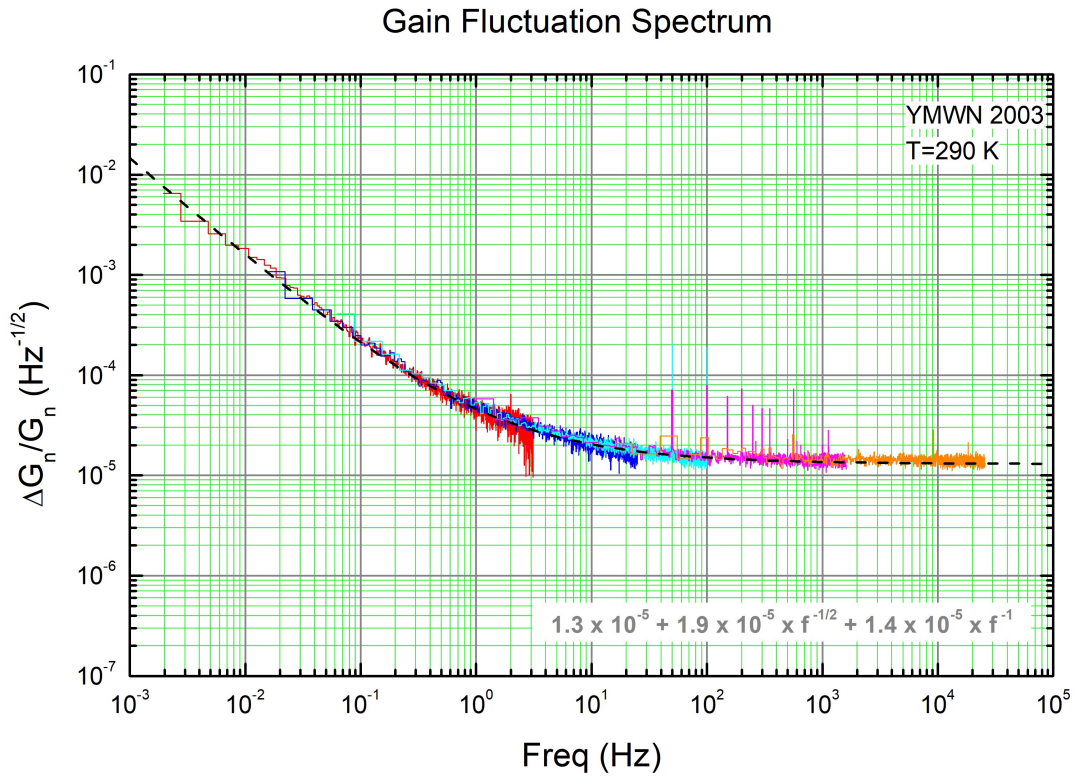


**Figure 5:** Results of the measured SNGF at ambient (up) and cryogenic (down) temperature. The fitting function is shown as the dashed black line. The cryogenic graph also present the colour coded background noise level introduced by the DC preamp and FFT analyzer in each frequency range and the level of white noise fluctuation due to the random nature of the input signal over the noise bandwidth of the measurement setup (dashed red line).

This limits also the confidence range of the Allan Variance calculated. It is shown in [2] that the time range for which the analytic expression is a good approximation can be obtained as:

$$\tau_{min} = \frac{1}{f_{max}} \quad ; \quad \tau_{max} = \frac{0.06}{f_{min}}$$

Figure 6 presents the graph of the Allan Variance obtained in this way. The red curve represents the value obtained by transformation of the SNGF of present measurement. Two curves have been added to represent what is expected in the bandwidth of a channel of some spectral receivers of interest [3] [4]. Note that the minimum of the Allan variance shifts to larger integration times with the reduction of the noise bandwidth. The time for the minimum can be easily calculated by finding the root of the derivative of the expression of  $AVAR(\tau)$ . The result is:

$$\tau_{minAVAR} = \sqrt{\frac{6}{NBW} \frac{1}{2\pi c}}$$

Note that this is only dependant on the coefficient of the 1/f noise and the noise bandwidth.

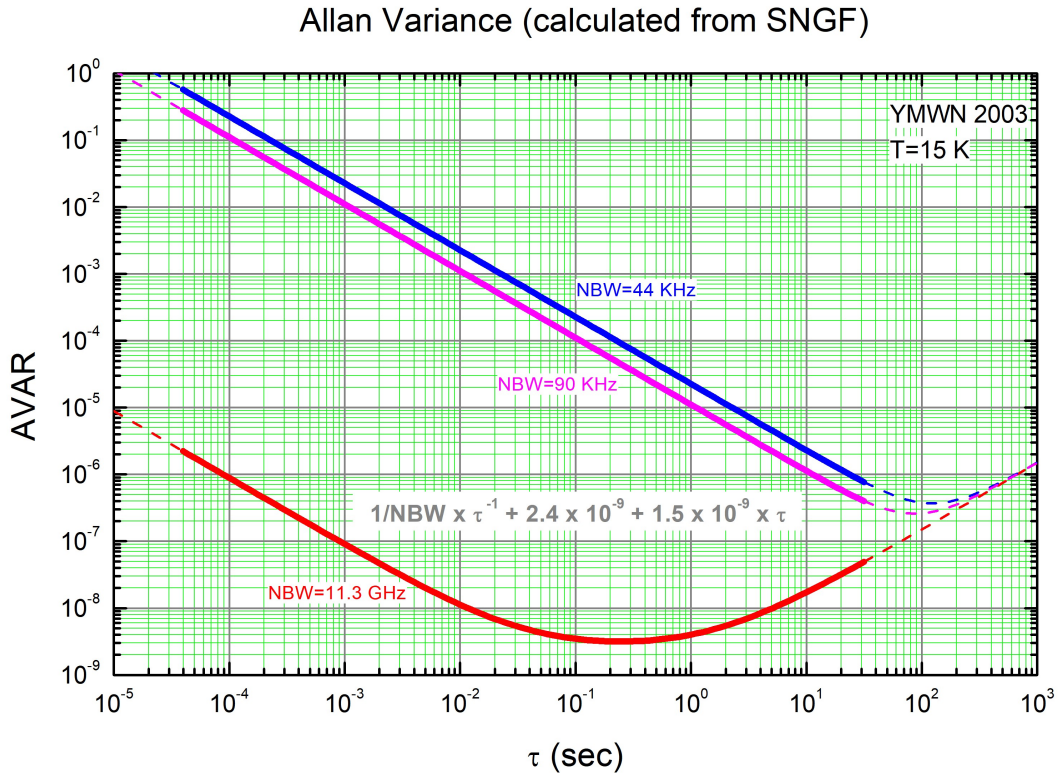


**Figure 6:** Allan Variance obtained by calculation from SNGF. The strict validity range (solid lines) is from  $4 \cdot 10^{-5}$  to 30 sec as given by the frequency range of the measurement of the SNGF. There are three curves calculated for different noise bandwidths: in red the value of the present measurement, in blue for the NANOCOSMOS FFT backend and in magenta for a hypothetical bandwidth optimized for the detection of axions in W band.

## 7. Conclusions

The Spectrum of Normalized Gain Fluctuation (SNGF) and the Allan Variance of the cryogenic W-band amplifier YMWN2003 have been measured at ambient and cryogenic temperature using a setup based on measuring the total output noise power with a matched input termination over a noise bandwidth determined mainly by the downconverter ( $\approx 11.3$  GHz centered on 95 GHz). The result can be fitted well by a function with terms of white,  $f^{-1/2}$  and  $f^{-1}$  noise. By the experience with measurements of other lower frequency amplifiers and by the values obtained it is believed that term of  $f^{-1/2}$  is dominated by the contribution of the cryogenic amplifier and its coefficient doubles at cryogenic temperature. It is not clear whether the  $f^{-1}$  term is due to the cryogenic amplifier or there is a significant contribution from the downconverter and the IF amplifier which could not be accounted for independently.

Overall, the values obtained can be considered acceptable although the Allan Variance appears to be larger than desirable for long integration times ( $>10$  sec). This is consequence of the high value of the  $f^{-1}$  term of the measured SNGF and as said before it is uncertain whether this is due to the unknown contribution of some components of the setup chain other than the amplifier tested. Note that, for example, the ALMA specification asks for values of  $\text{AVAR} < 2 \cdot 10^{-8}$  ( $0.05 < \tau < 100$  sec) and  $\text{AVAR} < 2 \cdot 10^{-7}$  ( $100 < \tau < 300$  sec). In our present measurement, the value of  $2 \cdot 10^{-8}$  is reached at  $\tau = 10$  sec due to the high value of the coefficient of the  $f^{-1}$  term.

## 8. References

- [1] I. Malo, J.D. Gallego, R. Amils, R. Garcia, M. Diez, I. López-Fernández, A. Barcia, “Improved Design of a Q band (33 50 GHz) Cryogenic Heated Load in Waveguide for Precision Noise Measurements with Reduced Heat Capacity,” CDT Technical Report 2016-6. <https://icts-yebes.oan.es/reports/doc/IT-CDT-2016-6.pdf>
- [2] J.D. Gallego, I. Lopez, C. Diez, A. Barcia, “Methods for the characterization and measurement of the gain fluctuations of cryogenic amplifiers,” ALMA memo #560 Nat. Radio Astron. Observatory, 2006 <http://legacy.nrao.edu/alma/memos/html-memos/alma560/memo560.pdf>
- [3] F. Tercero, J. A. López-Pérez, J. D. Gallego, F. Beltrán, O. García, M. Patino-Esteban, I. López-Fernández, G. Gómez-Molina, M. Diez, P. García-Carreño, I. Malo, R. Amils, J. M. Serna, C. Albo, J. M. Hernández, B. Vaquero, J. González-García, L. Barbas, J. A. López-Fernández, V. Bujarrabal, M. Gómez-Garrido, J. R. Pardo, M. Santander-García, B. Tercero, J. Cernicharo, P. de Vicente, “Yebes 40 m radio telescope and the broad band Nanocosmos receivers at 7 mm and 3 mm for line surveys,” *A&A* 645 A37 (2021). DOI: 10.1051/0004-6361/202038701.
- [4] B. Aja, S. A. Cuendis, I. Arregui, E. Artal, R. Belen Barreiro, F. J. Casas, M. C. de Ory, A. Díaz-Morcillo, L. de la Fuente, J. D. Gallego et al., “The Canfranc Axion Detection Experiment (CADEX): Search for axions at 90 GHz with kinetic inductance detectors,” *JCAP*11(2022)044, DOI 10.1088/1475-7516/2022/11/044. <https://arxiv.org/abs/2206.02980>

## 9. Appendix I: 8474C Diode Detector Data Sheet

### Product specifications

Model	Frequency (GHz)	Frequency response	Maximum SWR	Low level sensitivity (mV/μW)	Max operating input power	Typical short term maximum input power (< 1 minute)	Video impedance	RF bypass capacitance (nom)	Input connector	Output connector
8471D	0.01 to 2	± 0.2 to 1 GHz ± 0.4 to 2 GHz	1.23 to 1 GHz 1.46 to 2 GHz	> 0.5	100 mW	0.7 W	1.5 kΩ	6800 pF	BNC (m)	BNC (f)
8471E	0.01 to 12	± 0.23 to 4 GHz ± 0.6 to 8 GHz ± 0.85 to 12 GHz	1.2 to 4 GHz 1.7 to 8 GHz 2.4 to 12 GHz	> 0.4	200 mW	0.75 W	1.5 kΩ	30 pF	SMA (m)	SMC (m)
8473D	0.01 to 33	± 0.25 to 14 GHz ± 0.4 to 26.5 GHz ± 1.25 to 33 GHz ± 2.0 dB to 40 GHz	1.2 to 14 GHz 1.4 to 26.5 GHz 2.0 to 33 GHz 3.0 typical to 40 GHz	> 0.4	200 mW	1 W	1.5 kΩ	30 pF	3.5 mm (m)	BNC (f)
8474B	0.01 to 18	± 0.35 to 18 GHz	1.3 to 18 GHz	> 0.4	200 mW	0.75 W	1.5 kΩ	27 pF	Type-N (m)	BNC (f)
8474C	0.01 to 33	± 0.4 to 26.5 GHz ± 0.7 to 33 GHz	1.4 to 26.5 GHz 2.2 to 33 GHz	> 0.4 > 0.34 to 50 GHz	200 mW	0.75 W	1.5 kΩ	27 pF	3.5 mm (m)	SMC (m)
8474E	0.01 to 50	± 0.3 to 26.5 GHz ± 0.6 to 40 GHz ± 1.0 to 50 GHz	1.2 to 26.5 GHz 1.6 to 40 GHz 2.8 to 50 GHz	> 0.4 to 40 GHz	200 mW	0.75 W	1.5 kΩ	27 pF	2.4 mm (m)	SMC (m)